



OPEN ACCESS

EDITED BY

Yan Du,
University of Science and Technology
Beijing, China

REVIEWED BY

Qiang Guo,
China Jiliang University, China
Baiyu Chen,
University of California, Berkeley,
United States

*CORRESPONDENCE

Hongsheng Liu,
1769303449@qq.com

SPECIALTY SECTION

This article was submitted to
Environmental Informatics and
Remote Sensing,
a section of the journal
Frontiers in Environmental Science

RECEIVED 30 June 2022

ACCEPTED 24 August 2022

PUBLISHED 28 September 2022

CITATION

Jiang S, Liu H, Lian M, Lu C, Zhang S, Li J
and Li P (2022), Rock slope
displacement prediction based on
multi-source information fusion and
SSA-DELM model.
Front. Environ. Sci. 10:982069.
doi: 10.3389/fenvs.2022.982069

COPYRIGHT

© 2022 Jiang, Liu, Lian, Lu, Zhang, Li and
Li. This is an open-access article
distributed under the terms of the
[Creative Commons Attribution License
\(CC BY\)](https://creativecommons.org/licenses/by/4.0/). The use, distribution or
reproduction in other forums is
permitted, provided the original
author(s) and the copyright owner(s) are
credited and that the original
publication in this journal is cited, in
accordance with accepted academic
practice. No use, distribution or
reproduction is permitted which does
not comply with these terms.

Rock slope displacement prediction based on multi-source information fusion and SSA-DELM model

Song Jiang^{1,2,3}, Hongsheng Liu^{1,2*}, Minjie Lian^{1,4}, Caiwu Lu^{1,2}, Sai Zhang^{1,2}, Jinyuan Li^{1,2} and PengCheng Li⁵

¹Xi'an University of Architecture and Technology, School of Resources Engineering, Xi'an, China, ²Xi'an Key Laboratory of Smart Industry Perception Computing and Decision Making, Xi'an, China, ³Xi'an U-MINE Intelligent Mining Research Institute Co Ltd, Xi'an, China, ⁴Sinosteel Mining Development Co Ltd, Beijing, China, ⁵Jidong Cement Tongchuan Ltd., Tongchuan, China

In order to solve the inefficient use of multi-source heterogeneous data information cross fusion and the low accuracy of prediction of landslide displacement, the current research proposed a new prediction model combining variable selection, sparrow search algorithm, and deep extreme learning machine. A cement mine in Fengxiang, Shaanxi Province, was studied as a case. The study first identified the variables related to landslide displacement of rock slope, and removed redundant variables by using Pearson correlation and gray correlation analysis. To avoid the impacts of random input weights and random thresholds in the DELM model, the SSA algorithm is used to optimize the model's parameters, which can generate the optimal parameter combinations. The results showed an enhanced generalization ability of the model by removal of redundant variables by Pearson correlation and gray correlation analysis, and higher accuracy in the prediction of landside displacement of rock slope by SSA-DELM compared to other traditional machine learning algorithms. The current study is significant in the literature on rock slope disaster analysis.

KEYWORDS

multi-source data fusion, displacement prediction, SSA algorithm, deep extreme learning machine, variable selection

Introduction

In the construction of mountain housing, transportation, mining, water conservancy and hydropower projects, rock slope stability problems are inevitably encountered (Li et al., 2019; Du et al., 2022; Yi et al., 2022; Zhao et al., 2022). Rock slope stability problems can cause geological disasters such as rock loosening, relaxation cracking, creeping, landslides and rock fall (Liu et al., 2020; Meng et al., 2021; Xu et al., 2022). Therefore, monitoring and early warning are pivotal in preventing rock slope disasters. In rock slope disaster monitoring and early warning, the research is often conducted on static indicators (such as deformation, stress, etc.) or environmental indicators (such as groundwater,

rainfall, etc.) (Du et al., 2019), among which displacement is an intuitive and reliable monitoring quantity under the influence of internal and external environment. The scientific analysis of displacement data and the establishment of real-time prediction models are essential research contents in large-scale engineering safety monitoring.

In order to obtain accurate, comprehensive, and real-time information on landslide deformation, it is necessary to monitor both surface and subsurface deformation, as well as triggering factors and related environmental factors, so multiple means of landslide monitoring must be used simultaneously to achieve effective monitoring results (Zhang et al., 2020). Nowadays, the techniques applied in mainstream rock slope monitoring include synthetic aperture radar (Pieraccini et al., 2006; Atzeni et al., 2015; Qin et al., 2020), microseismic monitoring (Salvoni and Dight., 2016; Xu et al., 2016; Ma et al., 2017; Chen et al., 2022), GNSS displacement monitoring (Lian et al., 2020; Šegina et al., 2020; Yan et al., 2022), etc. These monitoring techniques mainly focus on the surface and deep deformation of rock slopes, and some scholars also combine environmental quantity indicators for monitoring and research, such as Pang (Pang, 2019) proposed an automated monitoring system, which contains GPS monitoring station, rain gauge, crack gauge, rain gauge, groundwater level gauge and other sensors to monitor the slope in real-time, which can respond to the slope deformation parts in time with a broader perspective to ensure the safety of high-risk slopes and their surroundings; Liu et al. (Liu et al., 2022) combined slope deformation monitoring data, displacement monitoring data, inclination monitoring data, groundwater level monitoring data, rainfall monitoring data and other multi-source data, based on machine learning method to monitor abnormal events of monitoring data to provide support for disaster early warning; Peng et al. (Peng et al., 2014) combined multiple sensor monitoring data and multiple mechanical parameters to update soil or rock model parameters, slope safety coefficients and damage efficiency using Markov chain Monte Carlo simulation, which made the assessment more reliable; Li et al. (Li et al., 2021) combined field experiments and blasting vibration monitoring to systematically study the three-dimensional dynamic stability of adjacent high slopes after blasting vibration, providing technical support and theoretical guidance for mine blasting and improving mine stability.

The use of multiple sensors to monitor slopes can obtain a large amount of multi-source heterogeneous data, which have specific correlation, randomness, and ambiguity (Wang et al., 2020). How to fully use these multi-source heterogeneous data is the focus of scholars' attention and the problems that have been needed. Over the past few years, the multi-source data fusion method has been increasingly favored by some experts and scholars in the field of slope research, and it has begun to be gradually applied in engineering. Some scholars have used multi-source data fusion technology for the prediction and stability

analysis of slope safety factor (Sakellariou and Ferentinou., 2005; Liu et al., 2014.; Jiang et al., 2022), and some scholars at home and abroad have used multi-source heterogeneous data fusion technology for risk warning and analysis of landslides to study the characteristic mechanism and dynamics evolution law of the deformation and damage process of landslides (Du et al., 2020; Zhang et al., 2020; Li et al., 2021). In recent years, multi-source data fusion techniques have been more successfully applied to landslide displacement prediction. Liu et al. (Liu et al., 2020) introduced two concepts, trend sequence and sensitivity, to quantitatively characterize landslide displacement caused by external factors and internal landslide state, respectively, and proposed a nonlinear model for landslide displacement prediction by fusing trend sequence and sensitivity state; Wang et al. (Wang et al., 2021) used Pearson correlation coefficient, and mutual information were used to screen environmental factors and deep learning was used to predict landslide displacements; Duan et al. (Duan et al., 2017) used comprehensive landslide monitoring data to extract the most relevant factors affecting landslide deformation and used an autoregressive integrated movement model for prediction. Wang and Zhang (Wang et al., 2022; Zhang et al., 2022) considered the hydrodynamic effects affecting landslides, used a variational modal decomposition method to decompose the cumulative displacement into the trend, periodic and stochastic terms, and used different deep learning methods to make predictions for three Different deep learning methods are used to predict the three different displacement subterms.

Scholars have rarely considered the relationship between the dependent variables in the prediction of landslide displacement using multi-source heterogeneous data of slopes, which can lead to overfitting and low prediction accuracy in the prediction. Nowadays, the mainstream methods of variable selection mainly include correlation analysis (Guo et al., 2022), mutual information (Li, 2021), and lasso (Jin et al., 2021). However, these methods are relatively single, and it is difficult to select the appropriate number of variables when screening the variables, and too few input variables will lead to lower prediction accuracy. On the other hand, too many input variables will result in redundant variables and increase the model running time.

In the past, scholars did not consider the redundancy among the dependent variables when using multi-source heterogeneous data of slopes for landslide displacement prediction, leading to overfitting and low prediction accuracy. To this end, this paper proposes a method of variable selection by combining Pearson correlation and gray correlation analysis. The Pearson correlation analysis is used to calculate the correlation coefficients of each variable factor, judging whether there are uncorrelated or redundant relationships among them. Then the model combines the correlation coefficients between variables and displacement to eliminate redundant variables. Finally, the sparrow search algorithm optimized by the depth limit learning machine is utilized to predict displacement, which provides a

TABLE 1 The value range of $|r|$ and its meaning.

The value range of $ r $	The meaning of $ r $
[0.0.2]	Extremely low correlation
[0.2.0.4]	Low correlation
[0.4.0.6]	Moderate correlation
[0.6.0.8]	High correlation
[0.8.1]	Extremely high correlation

reference for the subsequent displacement change and reduces the occurrence of slope disaster.

Principles of algorithms

Pearson correlation analysis

Karl Pearson introduced the Pearson correlation coefficient (PCC) in the 1880s. The correlation coefficient determines whether each input variable is closely correlated with each other, and if two variables are highly correlated with each other, they belong to duplicate features and can be removed to achieve de-duplication or dimensionality reduction (Lin et al., 2019). The Pearson correlation coefficient is then expressed as follows:

$$r = \frac{\sum_{i=1}^N (x_i - \bar{x})(y_i - \bar{y})}{\sqrt{\sum_{i=1}^N (x_i - \bar{x})^2 \sum_{i=1}^N (y_i - \bar{y})^2}} \quad (1)$$

Where r is the Pearson correlation coefficient; x_i is the different value corresponding to the variable x ; \bar{x} is the average of the variables x ; y_i is the different value corresponding to the variable y ; \bar{y} is the average of the variables y ; N is the number of variables. The value range of the correlation coefficient is $[-1.1]$. When $|r| > 0$, it is a positive correlation; conversely, it is a negative one. The magnitude of the absolute value of the corresponding Pearson correlation coefficient between two variables determines the strength of the relationship between the two variables, and the specific range of values and their representative meanings are shown in Table 1.

Gray relational analysis

Gray relational analysis theory, an essential part of gray system theory, is a multifactor statistical analysis theory that describes the strength, magnitude, and order among factors in terms of gray correlation degree based on sample data of each factor. Gray correlation is essentially a comparison of how close the geometric shapes of the data curves are. The closer the

geometry, the closer the trend of change and the greater the correlation (Liu et al., 2012). The analysis steps are as follows:

Step1. Identify the mother series and characteristic series. Generally, the dependent variable is determined as the mother series, and the independent variable is determined as the characteristic series. In this paper, the landslide displacement is determined as the mother series, and the landslide impact factor is determined as the characteristic series.

Step2. Undimensionalize the data. The dimensionless processing is typically done by initialization, homogenization, and normalization, and this paper uses normalization for the dimensionless processing of data. The calculation formula of normalization is then expressed as follows:

$$X_{\text{norm}} = \frac{X - X_{\text{min}}}{X_{\text{max}} - X_{\text{min}}} \quad (2)$$

Where X is the raw data; X_{max} , X_{min} are respectively the maximum and minimum values of the data.

Step3. Solve for the gray relational coefficient value between the parent sequence and the feature sequence. The relational coefficient represents the degree of correlation between the feature series and the mother series in the corresponding dimension, and the larger the number, the stronger the correlation. The calculation formula of the correlation coefficient is then expressed as follows:

$$\xi_e(k) = \frac{\min_e \min_k |x_0(k) - x_e(k)| + \rho \max_e \max_k |x_0(k) - x_e(k)|}{|x_0(k) - x_e(k)| + \rho \max_e \max_k |x_0(k) - x_e(k)|} \quad (3)$$

Where $\xi_e(k)$ is the value of correlation coefficients of feature sequence x_e to feature sequence x_0 on the k th indicator.

Step4. Calculate the correlation between the mother sequence and the feature sequence. Larger correlation degree proves that the corresponding feature sequence has more influence on the mother sequence. The calculation formula of correlation degree is then expressed as follows:

Where n is the sample size; r_e is the correlation degree of feature sequence, and the indicator weight.

$$r_e = \frac{1}{n} \sum_{k=1}^n \omega_k \xi_e(k) \quad (4)$$

Sparrow search algorithm

The Sparrow Search Algorithm (SSA) is a relatively novel algorithm inspired by the foraging and anti-predatory behaviors of sparrows (Xue and Shen., 2020), which has the advantages of

merit-seeking solid ability, fast convergence, and robustness. The bionic principle is as follows:

When sparrows search for food, they need to divide the whole sparrow population into three categories according to their different divisions of labor: producers searching for food, joiners grabbing food of their kind, and vigilantes finding enemies. Producers are generally the highest energy sparrows in the whole population because they need to search for food and guide the direction of the population. In continuous iteration, producers and joiners can transform each other, but the proportion of the two species in the whole population will not change in the transformation process. In the bionic experiment, the sparrow population and fitness values need to be initialized first, and the sparrow population and fitness value initialization expressions are then expressed as follows:

$$X = \begin{pmatrix} x_{1,1} & x_{1,2} & \cdots & x_{1,d} \\ x_{2,1} & x_{2,2} & \cdots & x_{2,d} \\ \vdots & \vdots & & \vdots \\ x_{n,1} & x_{n,2} & \cdots & x_{n,d} \end{pmatrix} \quad (5)$$

$$F_x = \begin{bmatrix} f([x1, 1 \ x1, 2 \cdots x1, d]) \\ f([x2, 1 \ x2, 2 \cdots x2, d]) \\ \vdots \\ f([xn, 1 \ xn, 2 \cdots xn, d]) \end{bmatrix} \quad (6)$$

Where n is the number of sparrows; d is the dimension of the variable to be optimized, which is the number of independent parameters; $x_{n,d}$ is the value of the n th sparrow in the d th dimension.

After determining the location and fitness value of each sparrow, the initial fitness value of each sparrow needs to be sorted, the sparrows with the better fitness value will be identified as the producer. The producer can be given priority to obtain food when food is found and guide the whole group to the direction of food. The producer will continue to search for food in different places elsewhere, the location will keep changing, and the movement rules will also change when the enemy is encountered, at the moment, the producer location update rules are then expressed as follows:

$$x_{i,j}^{t+1} = \begin{cases} x_{i,j}^t \exp\left(-\frac{i}{\alpha \text{iter}_{\max}}\right), & \text{if } R_2 < ST \\ x_{i,j}^t + QL, & \text{if } R_2 \geq ST \end{cases} \quad (7)$$

Where t is the current number of iterations; $j \in \{1, 2, 3, \dots, d\}$; $x_{i,j}^t$ is the value of the i th dimension of the j th sparrow at the t th iteration; $\alpha \in (0, 1]$, is a random number; iter_{\max} is the maximum number of iterations; $R_2 \in [0, 1]$, is the alarm value; $ST \in [0, 1]$, is the safety threshold; Q is a random number that follows a normal distribution; L is a matrix of order $1 \times d$ (all elements are 1). When $R_2 < ST$, it means that there are no natural predators in the area, which means that the area is safe and the producer will continue to expand its foraging range; when $R_2 > ST$, it means

that the producer has found a predator and warned other sparrows that all sparrows need to leave the area for a safe area.

For the joiners, the producers are monitored at all times, and if the producers find food, the joiners will immediately be aware of it and quickly fly to the food source to grab the food with the producer. At this time, the joiners' position update rule is then expressed as follows:

$$x_{i,j}^{t+1} = \begin{cases} Q \exp\left(\frac{x_{\text{worst}}^t - x_{i,j}^t}{t^2}\right), & i > \frac{n}{2} \\ x_p^{t+1} + |x_{i,j}^t - x_p^{t+1}| A^+ L, & \text{else other} \end{cases} \quad (8)$$

Where x_p is the best position occupied by the producer; x_{worst} is the global worst position; A is the matrix of order $1 \times d$, each element is randomly 1 or -1; $A^+ = A^T (AA^T)^{-1}$; When $i > \frac{n}{2}$ it means that the less adaptive first joiner fails to grab food and needs to change its position to get food in other areas.

Alerters are randomly generated in the entire population, usually 10–20% of the entire population. The initial position is then randomly generated, with the rule is then expressed as follows:

$$x_{i,j}^{t+1} = \begin{cases} x_{\text{best}}^t + \beta |x_{i,j}^t - x_{\text{best}}^t|, & \text{if } f_i > f_g \\ x_{i,j}^t + K \left(\frac{|x_{i,j}^t - x_{\text{worst}}^t|}{(f_i - f_w) + \varepsilon} \right), & \text{if } f_i = f_g \end{cases} \quad (9)$$

Where f_i is the current sparrow adaptation value; f_g is the global best adaptation value; f_w is the global worst adaptation value; β is the step control function, which is a normally distributed random number with mean 0 and variance 1; K is the direction of sparrow movement; ε is the minimum constant, avoiding zero denominator; x_{best} is the global best position; x_{worst} is the global worst position. When $f_i > f_g$, it means that the vigilantes are located at the edge of the whole population and will fly to the safe area when scouting for enemies; When $f_i = f_g$, it means that the vigilantes in the centre of the population are aware of the danger and will fly to the other sparrows to avoid the danger.

Deep Extreme Learning Machine

An extreme learning machine is a single hidden layer feedforward neural network (Sulandri et al., 2021). Unlike the traditional gradient-based feedforward neural network algorithm, the input weights and thresholds of the hidden layer of the extreme learning machine network are randomly generated in the training process. Therefore, only the generalized inverse matrix theory can be used to calculate the output weights to complete the learning. Therefore, ELM network has the advantages of fast learning speed and strong generalization ability. However, because ELM is a single hidden layer

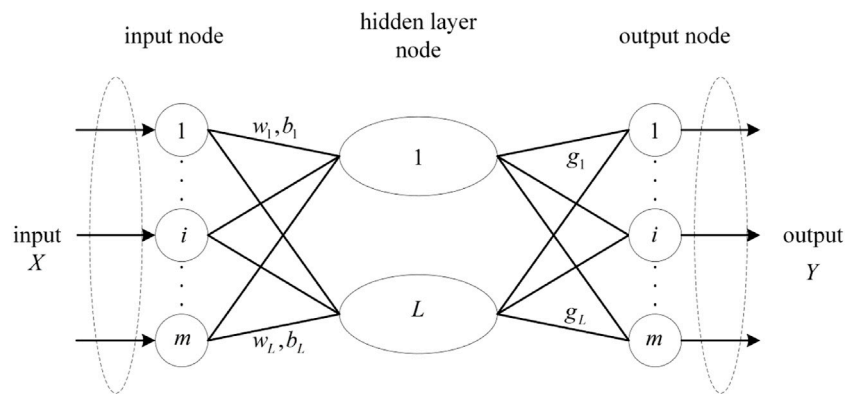


FIGURE 1
ELM-AE network structure diagram.

structure, it cannot capture the effective features of the data in the case of high data, and high dimensionality of data. So more scholars use DELM (Tuerxun et al., 2021), which is a derivative algorithm of ELM.

Deep Extreme Learning Machine (DELM) is an ELM derivative algorithm that improves the network’s representational capability by superimposing an Extreme Learning Machine-Autoencoder (ELM-AE) to construct a multilayer network structure. When the ELM is confronted with input and output variables with an excessive amount of input data and high dimensionality, it solves the problem that an extreme learning machine with only one hidden layer cannot capture the effective features of the data (Sulandri et al., 2021). DELM is a combination of an extreme learning machine and an autoencoder, which constitutes an extreme learning machine-autoencoder, and the ELM-AE structure is shown in Figure 1.

ELM-AE is a general approximator characterized by enabling the output of the network to be the same as the input and the input parameters of the hidden layer to be orthogonal after random generation. The output of ELM-AE can be then as follows:

$$x_j = \sum_{i=1}^L \beta_i G(a_i, b_i, x_j), a_i \in R^m, \beta_i \in R^m, j = 1, 2, \dots, N, a^T a = I, b^T b = 1 \tag{10}$$

Where a is the matrix composed of a_i , and b is the vector composed of b_i . The output weights of the hidden layer are then expressed as follows:

$$\beta = \left(\frac{I}{C} + H^T H \right)^{-1} H T X \tag{11}$$

Where $X = [X_1, X_2, X_3, \dots, X_N]$ is the input data.

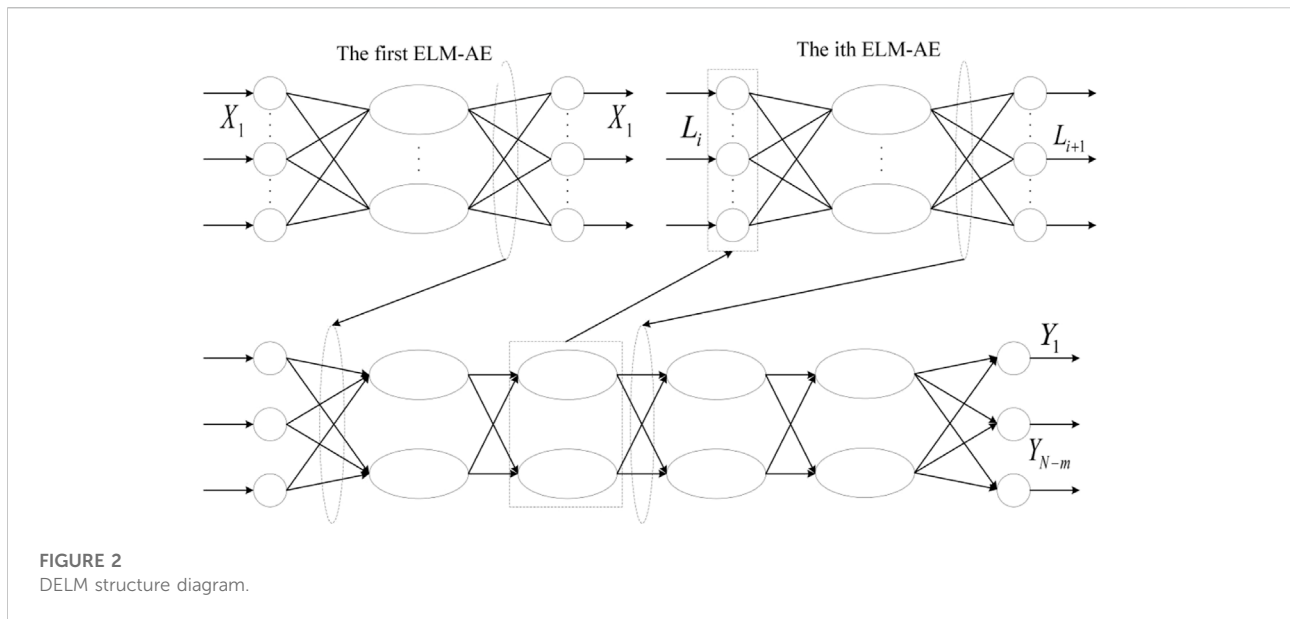
Because of its feature representation capability, ELM-AE is used as the basic unit of the deep extreme learning machine

DELM. Like traditional deep learning algorithms, DELM also uses a layer-by-layer greedy training method to train the network, and the input weights of each hidden layer of DELM are initialized using ELM-AE to perform hierarchical unsupervised training, but unlike traditional deep learning algorithms, DELM does not need reverse fine-tuning process. The structure of DELM is shown in Figure 2.

Assuming that the model has N hidden layers, the first output weight matrix β_1 is obtained from the input data X according to ELM-AE theory and then the feature vector of the hidden layer H^1 . The output weight matrix β_N of N layers and the feature vectors H^N of the hidden layers can be obtained. As shown in Figure 3, the DELM first uses multiple ELM-AEs for unsupervised pre-training and then uses the output weights of each ELM-AE to initialize the whole DELM. During the ELM-AE training process, the input layer weights and thresholds are randomly generated orthogonal random matrices; meanwhile, the ELM-AE unsupervised training process uses the least squares method to update the parameters. However, in this process, only the output layer weight parameters are updated, while the input layer weights and thresholds are fixed, which will result in the prediction accuracy of the DELM being affected by the random input weights and random thresholds of each ELM-AE. Therefore, it is necessary to optimize these two parameters.

Establishment of SSA-DELM predict model

Multiple ELM-AEs stack DELM, and the input weights and random thresholds in ELM-AEs are randomly generated, leading to random variables in the DELM model and unstable results. So these two parameters are iteratively optimized by the SSA algorithm, giving the whole model high prediction accuracy



and fast convergence, which can well ensure the stability of the results. The optimization process and flow chart (Zeng et al., 2021) are then as follows.

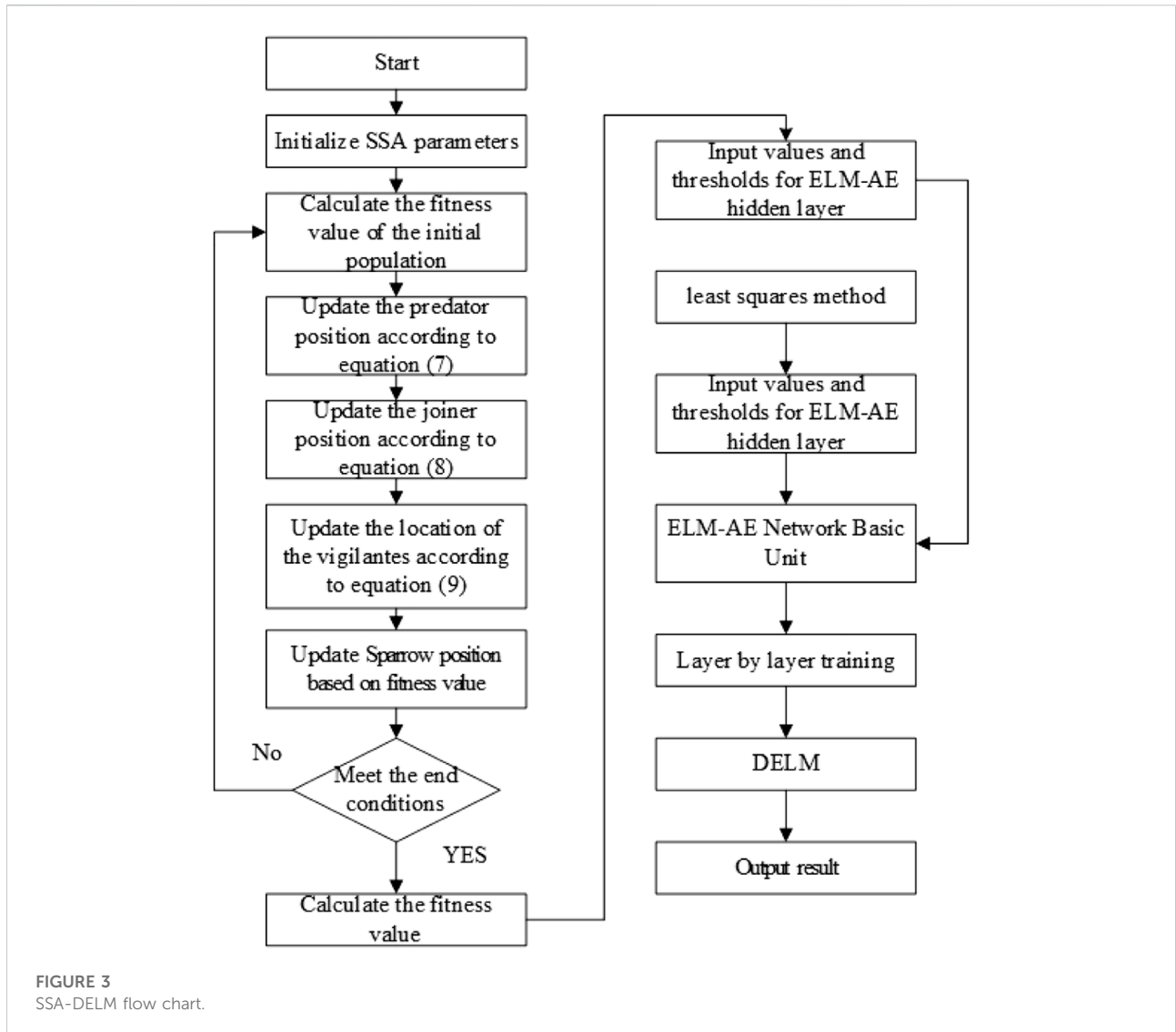
- 1) Initialize the SSA algorithm parameters. Set the maximum number of training iterations, the number of sparrow populations, the alert threshold, the proportion of discoverers, and the proportion of alerters.
- 2) Calculate the initial fitness value of the sparrow population. Then, the sparrows with the current best and worst fitness values are selected along with their locations.
- 3) The positions of predators, joiners, and vigilantes are continuously updated according to Eqs 7–9.
- 4) After updating the positions, calculate the optimal and worst fitness values of the whole population and their positions, determine whether the maximum number of iterations is satisfied or the stopping condition is met, and if the condition is fulfilled, output the optimal value, otherwise, return to step 2).
- 5) The obtained results are input into the DELM model to calculate the input values and thresholds of the optimal hidden layer.

Landslide displacement modeling based on PCC-GRA-SSA-DELM

There are various manifestations of rock slope deformation, and landslide displacement is one of them. In this paper, we will combine actual engineering cases and literature, collect multiple sensor data and multiple environmental factors affecting rock slope displacement as

the input parameters of SSA-DELM prediction model, and take displacement as the output parameters of the model. Since the redundancy among the factors will reduce the accuracy of the prediction model, this paper uses Person correlation analysis to calculate the correlation coefficients of the influencing factors. It then uses gray correlation analysis to calculate the correlation between the influencing factors and the landslide displacements to eliminate redundant and uncorrelated variables between them. The screened out in the prediction model, the rock slope displacement prediction model based on the PCC-GRA-SSA-DELM model is established based on four steps: data collection, data processing, variable selection, and result prediction. In this case, the obtained results are more accurate. The calculation process (as shown in Figure 4) is as follows:

- 1) Data collection. Multiple data sources are collected from the slope monitoring system, including displacement data, meteorological data, mechanics-related data, etc.
- 2) Normalizing the experimental data. Normalization limits the preprocessed data to a certain range eliminates the undesirable effects caused by odd sample data and performs inverse normalization after the model output results.
- 3) Variable selection. The correlation coefficients of the influencing factors were firstly calculated by using Person correlation analysis to judge the redundancy degree among the factors, and then the correlation degree between the influencing factors and landslide displacement was calculated by using gray correlation analysis, and the redundant variables and unrelated variables among them were eliminated by comprehensive comparison.



- 4) Result prediction. The samples are applied in the trained SSA-DELM model, the predicted values are output, and the feasibility and accuracy of the results are analyzed and verified.
- 5) Evaluation metrics. In this paper, the mean absolute error (MAE), and the mean square error (RMSE) are taken as the evaluation indexes of the model and calculated as follows:

$$X_{MAE} = \frac{1}{N} \sum_{i=1}^N |\hat{y}_i - y_i| \quad (12)$$

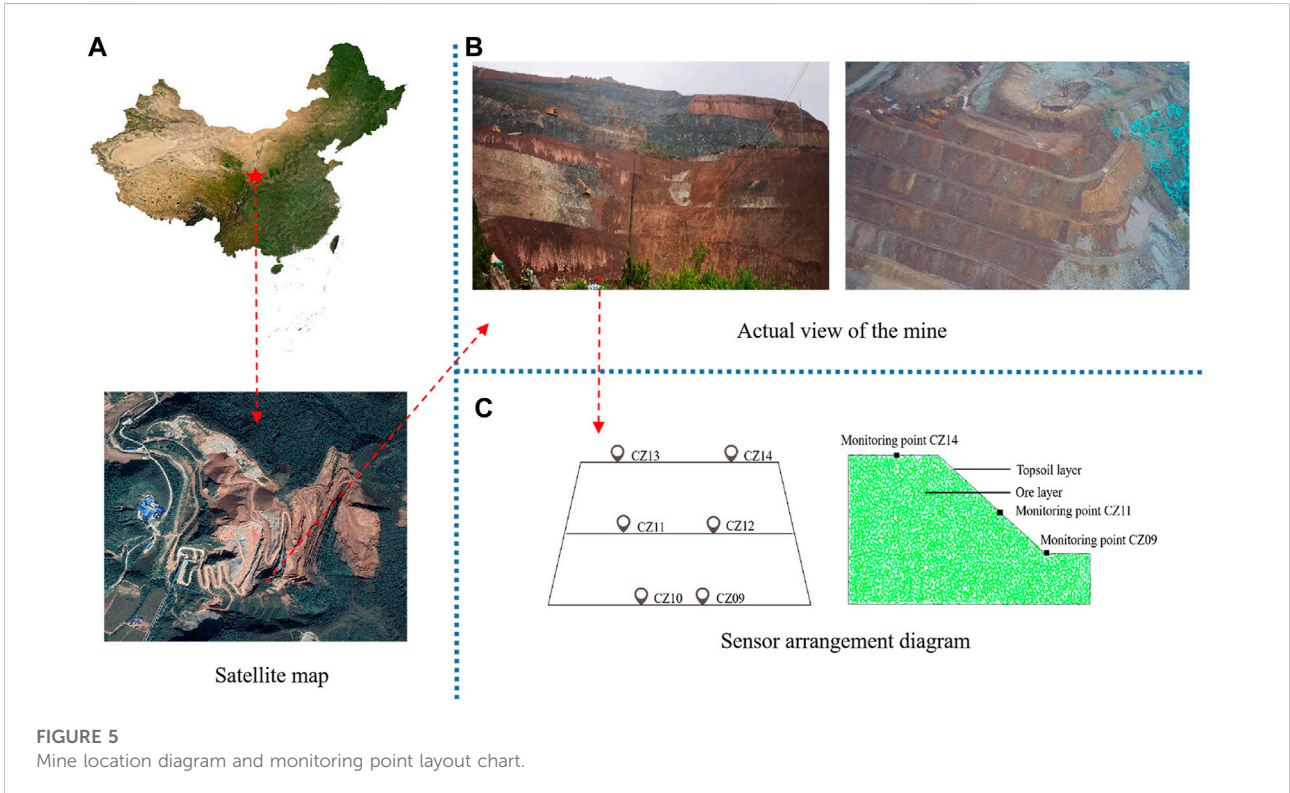
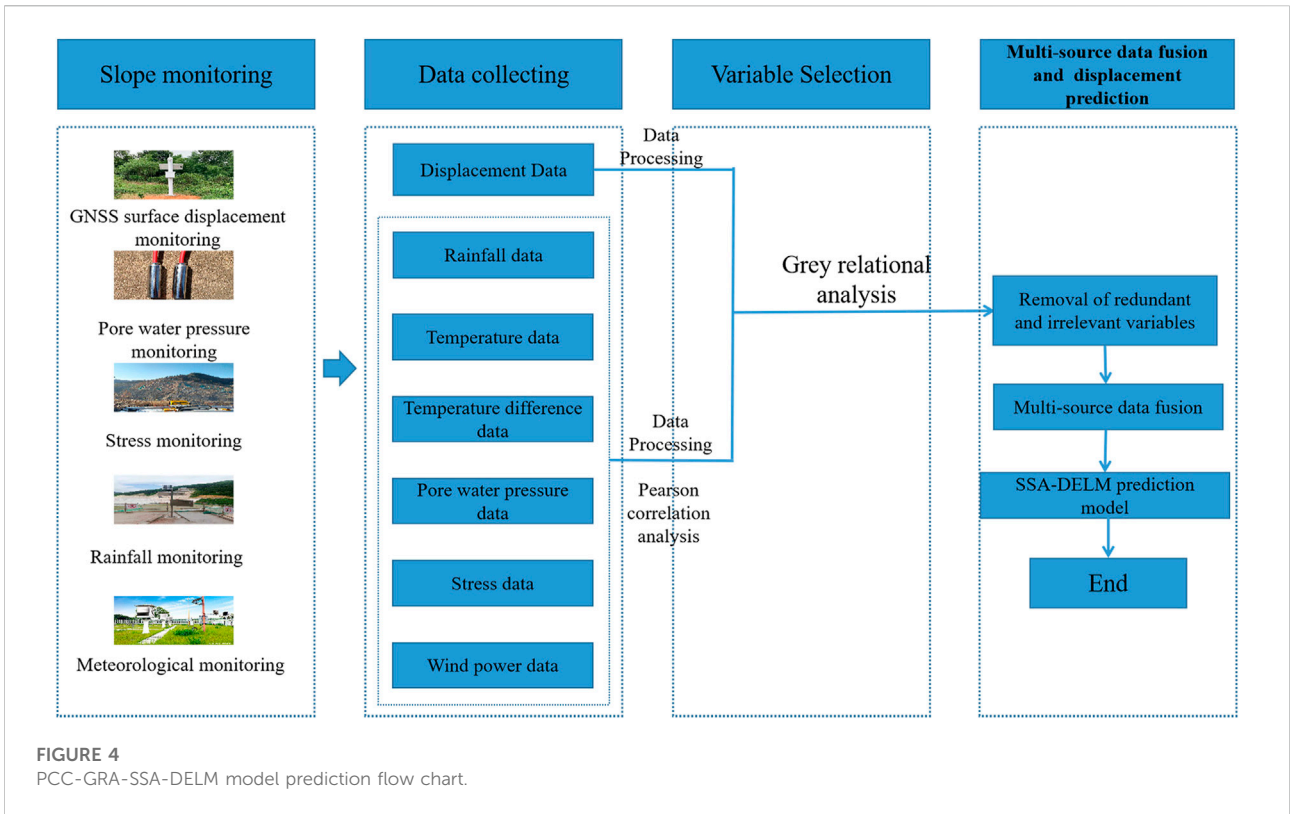
$$X_{RMSE} = \sqrt{\frac{1}{N} \sum_{i=1}^N |\hat{y}_i - y_i|^2} \quad (13)$$

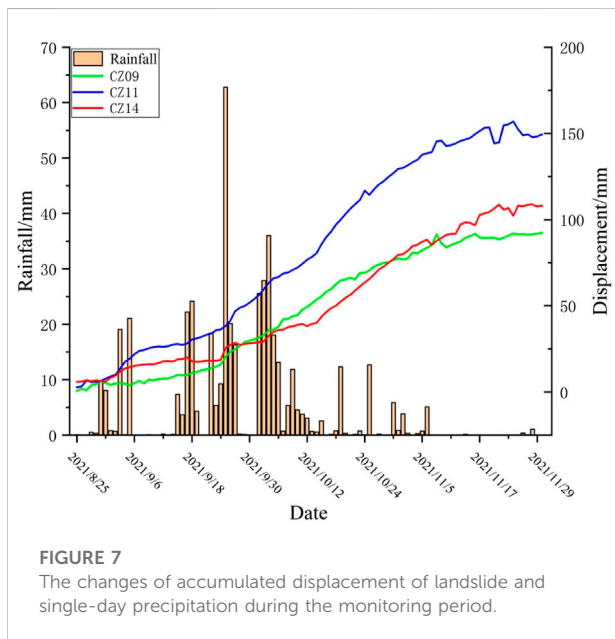
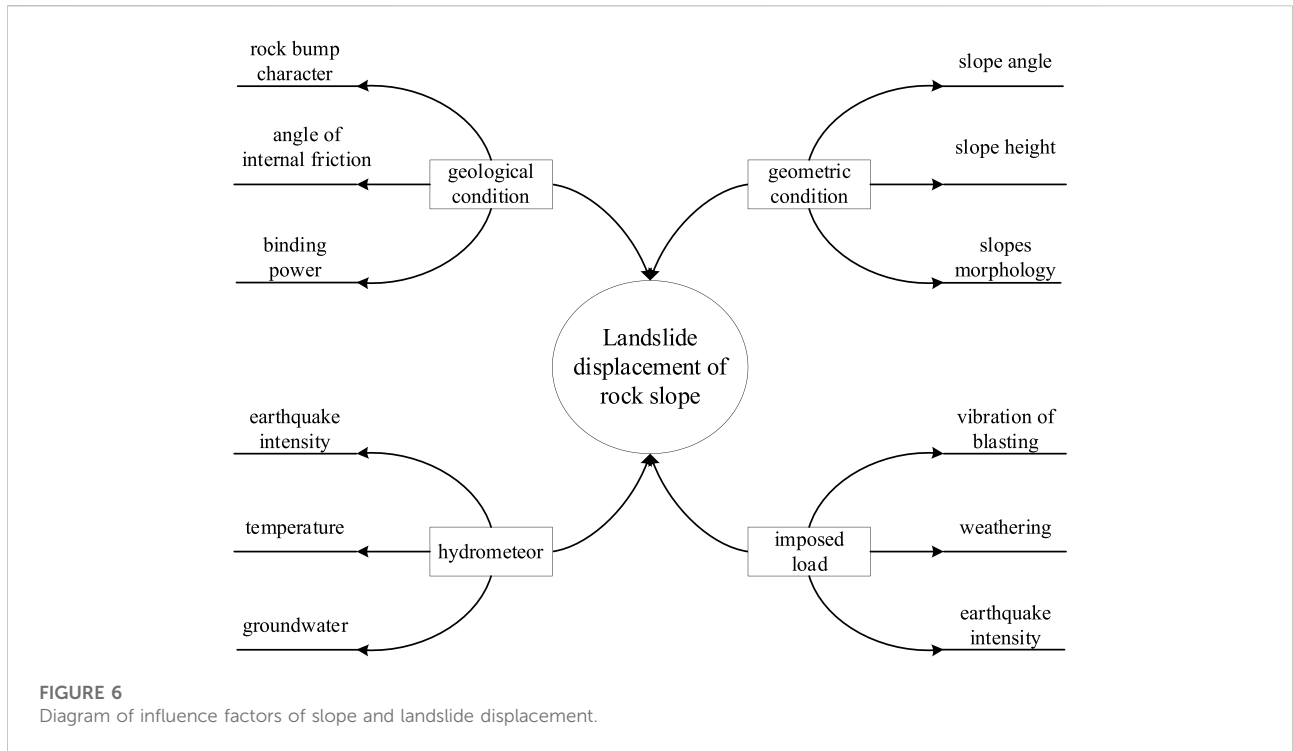
Where N is the number of samples predicted; y_i is the actual value of displacement; \hat{y}_i is the predicted value of displacement.

Numerical calculation and analysis

Introduction of case projects

A cement mine in Fengxiang District is located in Fengxiang District, Baoji City, Shaanxi Province, China, at latitude $34^{\circ}32'43''$ - $34^{\circ}32'54''$ N and longitude $107^{\circ}30'26''$ - $107^{\circ}30'57''$ E. The quarry slope is mainly composed of the Devonian medium-thick laminated hard tuff rock group, with tangential slope and reverse slope, which is more favorable to the stability of the slope, with good stability of the slope in general, and not easy to produce large-scale landslide, collapse and other geological disasters. On the other hand, the structure of the upper residual slope and weathered, broken layer is loose, with poor stability, which is prone to small-scale collapse and landslide geological disasters under rainfall and vibration.





When the mine started to be mined, the relevant management department continuously monitored the slope deformation, mainly including GNSS surface displacement, stress meter, pore water pressure meter, etc. The location map of GNSS surface displacement monitoring points is shown in

Figure 5, which includes two base stations (JZ01 and JZ02) and 14 observation stations. This paper selects three monitoring points CZ14, CZ11 and CZ09 in base station JZ02 located in the west section of the mine. These three monitoring points are located at the slope’s top, middle and foot in the west section of the mine, representing the deformation characteristics and trends of the front, middle and back of the slope.

The stability of rock slope is influenced by a variety of factors, which are mainly divided into four categories: engineering geology, geometric conditions, hydro-meteorology, and applied loads (as shown in Figure 6). Among them, rainfall is one of the critical factors affecting landslide deformation, and the changes in accumulated displacement of landslides and single-day precipitation during the monitoring period are shown in Figure 7. Temperature is one of the main factors affecting the mechanical properties of rocks (Li et al., 2022), and Weathering is the effect of changing the physical properties and chemical composition of rocks under atmospheric conditions. When other factors work together to a certain extent, it is very easy to cause slope instability, such as landslides, cave-ins, and other geological disasters, and rainfall, atmospheric radiation, temperature, and temperature difference are the main reasons affecting the weathering of rock slope. By geological survey of the mine site as well as its surrounding geology and literature query, the mine is divided into two segments, the left side of the western

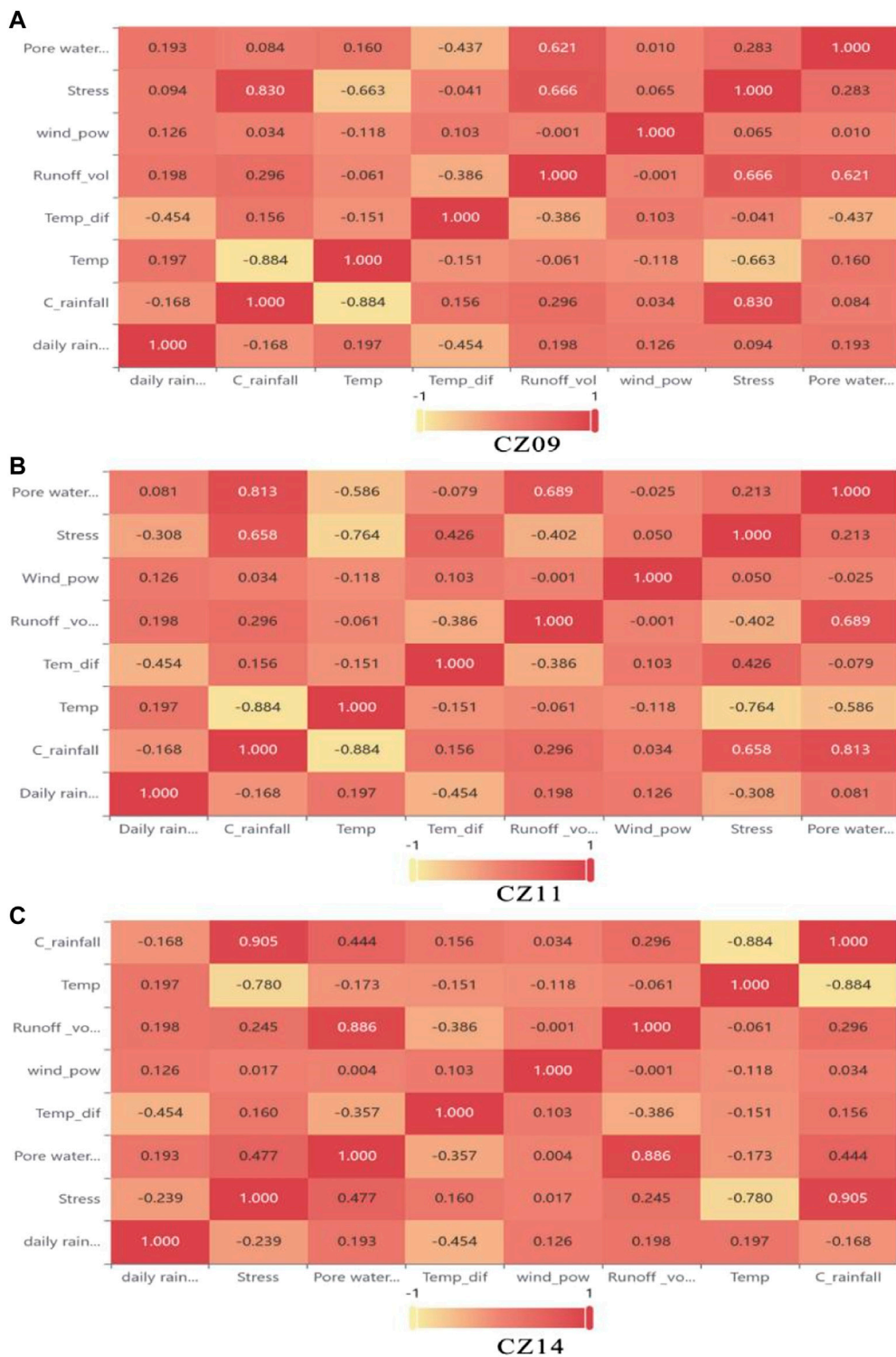


FIGURE 8 Correlation coefficient of three monitoring points influence factor (A) CZ09, (B) CZ11, (C) CZ14.

section is close to the Heng Shui River, and there is a tributary inflow, the size of the runoff from the Heng Shui River also affects the height of the groundwater level in the mine area, the

rise and fall of the groundwater level cause the slope geotechnical body to produce deformation, slippage, collapse instability and other adverse geological

TABLE 2 The correlation between the influence factors of the three monitoring points and the displacement.

Monitoring points	Cumulative rainfall	Runoff volume	Porewater pressure	Stress	Temperature	Wind power	Temperature difference	Daily rainfall
CZ09	0.971	0.889	0.911	0.917	0.856	0.907	0.918	0.831
CZ11	0.973	0.894	0.926	0.957	0.864	0.914	0.923	0.832
CZ14	0.958	0.886	0.912	0.922	0.861	0.909	0.921	0.829

TABLE 3 Error analysis table of 3 monitoring points.

Predictive model	CZ09		CZ11		CZ14	
	MAE	RMSE	MAE	RMSE	MAE	RMSE
PCC-GRA-SSA-DELM	1.3	1.75	1.06	1.44	1.19	1.68

phenomena, the groundwater level monitoring is mainly by means of pore water pressure sensors and stress gauges. Considering the above and the lag of some environmental impact factors on rock slope, the factors selected in this paper are daily rainfall (mm), accumulated rainfall (mm), daily average temperature (°C), daily temperature difference (°C), stress (Kpa), pore water pressure (Kpa), runoff (km), wind speed (m/s), among which the data of six factors such as rainfall, temperature, runoff and wind speed come from the meteorological monitoring station in Fengxiang District, Baoji City, Shaanxi Province. The stress and pore water pressure data comes from the measurement data of mine monitoring points.

Influencing factors selection

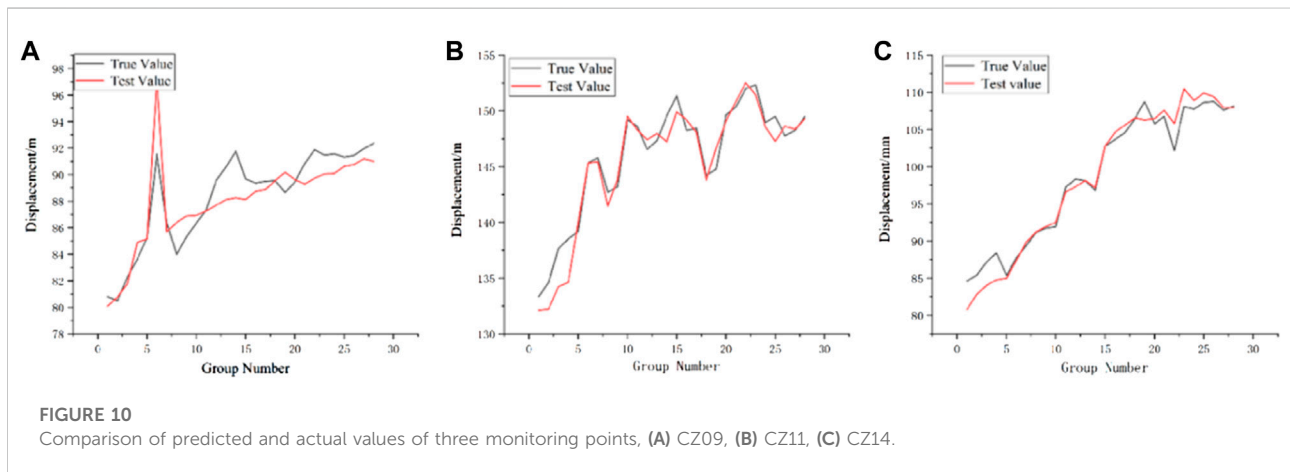
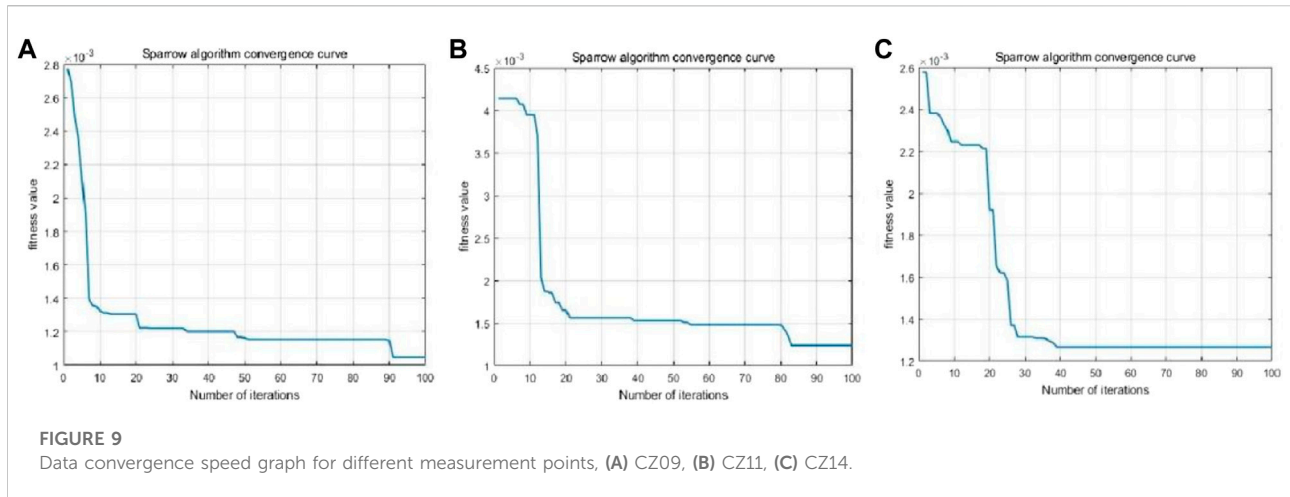
Pearson correlation analysis was performed on the eight influencing factors, and their correlation coefficients were calculated (Figure 8). Taking the correlation analysis of impact factors of the monitoring point CZ11 as an example, The correlation coefficients between cumulative rainfall and pore water pressure, temperature and stress were 0.815, -0.884 and 0.658, respectively, while the correlation coefficients between runoff and pore water pressure were, 0.680 and between temperature and stress were -0.764, respectively. It shows a very high degree of correlation with a close relationship. In summarizing, all eight influence factors have a certain correlation with each other, which proves that there is redundancy among the data, and if the prediction is directly fused, the prediction performance of the prediction model will be affected to some extent. Therefore, this section calculated the correlation between each influence factor and landslide

displacement using gray correlation analysis combined with the actual data from the experiment. The main influence factors were derived as the input variables of the prediction model (as shown in Table 2).

Taking monitoring point CZ11 as an example for analysis, combining Pearson correlation analysis and gray relational analysis for variable selection. Among the eight influencing factors, the top three correlations with landslide cumulative displacement are cumulative rainfall, stress, and pore water pressure, which are 0.973, 0.957, and 0.926, respectively. However, the correlation coefficients of cumulative rainfall and pore water pressure and stress are relatively large and strongly correlated. The two indicators of pore water pressure and stress are excluded, and the remaining six influencing factors are selected as input variables. Similarly, In monitoring points CZ09 and CZ14, the gray correlation between cumulative displacement and influence factors is greater for cumulative rainfall, stress, and temperature difference. However, since the correlation coefficients between cumulative rainfall and stress and temperature are higher, the two variables of stress and temperature are excluded, and the remaining six variables are retained as input variables.

Landslide displacement prediction

In the present study, the actual monitoring data of the Fengxiang cement mine from 25 August 2021, to 30 November 2021, are used as the experimental data, and there are 98 sets of valid data in total. As the slope has different responses to external influences at different locations, three sensors at different locations of the same slope will be selected for this experiment. The surface displacement data from



each sensor will be predicted, the first 70 sets of data from each sensor will be selected as the training sample set, and the last 28 monitoring data will be used as the prediction sample set.

The parameters of the SSA-DELM method were set as follows: the population size of sparrows was 100; the proportion of discoverers was 0.7, and the proportion of vigilantes was 0.2; the hidden layer of the DELM model was set to 4 layers, the number of nodes in each implicit layer was set to 10, and the maximum number of iterations was 100; the excitation function was selected as sigmoid, and the excitation function was able to achieve nonlinear transformation in the feature space, and the SSA algorithm to optimize the implied layers and input thresholds of DELM. The convergence speed is shown in Figure 9, and it can be seen that the SSA-DELM model converges within 100 iterations, and the fitness values can all be maintained at about 1.2×10^{-3} , indicating that the model converges quickly and has high prediction accuracy. The influence factors screened in the above section are used as input

parameters and the accumulated displacement as output parameters.

As shown in Table 3, the displacement prediction errors at three different locations are relatively small by using the PCC-GRA-SSA-DELM prediction model, among which, the smallest RMSE and MAE is monitoring point CZ11 with RMSE of 1.44. From the plots (b) and (c) in Figure 10, it can be seen that the predicted displacement trends of monitoring point CZ11 and monitoring point CZ14 are the same as the actual displacement trends. Basically, the larger errors are in the first five groups of the test set. Besides, their actual values of them are larger than the predicted values. Accidental loads or human activities during the mining can cause this phenomenon. Monitoring point CZ09 has the largest RMSE and MAE, and the points with larger errors are basically located in the second half of the test set, which is attributed to the fact that monitoring point CZ09 is located at the foot of the slope, and the accidental displacements

TABLE 4 Comparison of errors of different prediction models.

Predictive model	CZ09		CZ11		CZ14	
	MAE	RMSE	MAE	RMSE	MAE	RMSE
PGSD	1.3	1.75	1.06	1.44	1.19	1.68
SSA-DELM	1.57	1.80	3.26	3.68	2.95	3.47
ELM	7.25	11.33	7.21	8.65	6.94	9.28
SVM	12.25	15.3	8.46	9.55	2.98	4.19
DELM	7.26	7.86	5.98	6.43	5.47	6.24

generated by mining activities and vehicle transportation will affect the accuracy of displacement prediction. In conclusion, the overall effect of the PCC-GRA-SSA-DELM prediction model is excellent and can be applied to the actual landslide displacement prediction.

Comparison verification

In order to verify the supremacy of the proposed model in this paper, a support vector machine (SVM), extreme learning machine (ELM), deep extreme learning machine (DELM), and SSA-DELM were built in Matlab to conduct comparison experiments with this paper's model PCC-GRA-SSA-DELM (referred to as PGSD in the table) respectively. The prediction results of three different location sensors are shown in Table 4, among which the robustness of the ELM model is lowest.

The comparison experiments use MAE and RMSE as evaluation indicators, where the smaller the two values are, the better their prediction. Among them, ELM has the lowest prediction accuracy compared with the other two derived algorithms, DELM and SSA-DELM. DELM has more ELM-AEs than ELM, which increases the stability and merit-seeking ability of the model. However, during the ELM-AE training process, the input layer weights and thresholds are randomly generated orthogonal random matrices in the DELM model. The ELM-AE unsupervised training process uses least squares to update the parameters. Only the output layer weights parameters are updated, while the input layer weights and thresholds are fixed. That means the prediction accuracy of DELM is affected by the random input weights and random thresholds of each ELM-AE. But the SSA can solve this problem. Therefore, SSA-DELM has the highest prediction accuracy. The PGSD model proposed in this paper reduces the dimensionality of input variables, removes strongly correlated variables, enhances of the relationship between input and output variables, avoids overfitting, and improves the overall model prediction accuracy. Compared to SSA-DELM, the results showed the accuracy by the PGSD

model increased by 2.86, 60.8, and 51.59% at three different measurement points, respectively.

Conclusion

The present work combined variable selection and sparrow search algorithm-deep extreme learning machine algorithm to predict landslide displacement. The results were validated using monitoring data for a cement mine in Baoji City. The main findings of the study are summarized as follows:

- 1) The advantage of the variable selection is that it can remove redundancy between multi-variables and eliminate multicollinearity problems. The Pearson correlation analysis method identified the correlation coefficients between each variable. The magnitude of the correlation coefficients can be used to identify the redundancy between the variables. By combining with gray correlation analysis, the correlation between each input variable and the displacement can be calculated to eliminate the redundant variables and improve the accuracy of the prediction model.
- 2) The paper selected the locations of monitoring points at different locations of the same mine slope for the study. As a result, the correlation coefficients between landslide displacements and impact factors are different for different monitoring points, and the redundant and redundant variables to be eliminated are also different.
- 3) The PCC-GRA-SSA-DELM prediction model has a high predictive effect, and the overall effectiveness of fitting on three different monitoring points is strong, which can meet the demands of practical mine monitoring and early warning.
- 4) Compared with ELM, DELM and SVM traditional prediction algorithms, the PCC-GRA-SSA-DELM prediction model proposed in the research has higher prediction accuracy and prediction efficiency in rock slope landslide displacement prediction. Therefore, it is more suitable for the prediction of rock slope displacement.

In sum, the PCC-GRA-SSA-DELM fusion model proposed in this paper enriches the literature on the reliability of rock slope landslide monitoring and warning. The current research also has limits because the errors in original data caused by arbitrary factors, such as mining work, and human activities, are not considered. Therefore, future works can further focus on predicting periodic and trend term displacement by using the signal decomposition method to further enhance accuracy and reliability.

Data availability statement

The original contributions presented in the study are included in the article/Supplementary Material, further inquiries can be directed to the corresponding author.

Author contributions

SJ provided the ideas and framework for this study, including the methods and theories in the paper; HL, conducted the experiments and wrote this paper; ML, CL, and SZ, performed the preliminary reading of the first draft and gave critical comments; JL, assisted in the data processing and data analysis of this paper; PL, provided the test site and raw data, including the geographic location map of the mine, sensor data, etc. for this paper.

Funding

This work was supported by the research project of National Natural Science Foundation of China: Disaster identification and early warning of complex slope in open pit mine based on data knowledge hybrid drive (52104146); And the research project of Shaanxi Natural Science Foundation: Research on driverless

vehicle road collaborative intelligent control system in open pit mine integrating 5G Technology (2021JQ-509); And Shaanxi Social Science Foundation: Research on intelligent comprehensive perception and disaster emergency decision-making of National Central Cities Based on big data (2020R005).

Conflict of interest

Author SJ was employed by the company Xi'an U-MINE Intelligent Mining Research Institute Co Ltd, Author ML was employed by the company Sinosteel Mining Development Co Ltd, and Author PL was employed by the company Jidong Cement Tongchuan Ltd.

The remaining authors declare that the research was conducted in the absence of any commercial or financial relationships that could be construed as a potential conflict of interest.

Publisher's note

All claims expressed in this article are solely those of the authors and do not necessarily represent those of their affiliated organizations, or those of the publisher, the editors and the reviewers. Any product that may be evaluated in this article, or claim that may be made by its manufacturer, is not guaranteed or endorsed by the publisher.

Supplementary material

The Supplementary Material for this article can be found online at: <https://www.frontiersin.org/articles/10.3389/fenvs.2022.982069/full#supplementary-material>

References

- Atzeni, C., Barla, M., Pieraccini, M., and Antolini, F. (2015). Early warning monitoring of natural and engineered slopes with ground-based synthetic-aperture radar. *Rock Mech. Rock Eng.* 48, 235–246. doi:10.1007/s00603-014-0554-4
- Chen, J., Zhu, C., Du, J. S., Pu, Y. Y., Pan, P. Z., Bai, J. B., et al. (2022). A quantitative pre-warning for coal burst hazard in a deep coal mine based on the spatio-temporal forecast of microseismic events. *Process Saf. Environ. Prot.* 159, 110. doi:10.1016/j.psep.2022.01.082
- Du, Y., Li, H., Chicas, S. D., and Huo, L. C. (2022). Progress and perspectives of geotechnical anchor bolts on slope engineering in China. *Front. Environ. Sci.* 10. doi:10.3389/fenvs.2022.928064
- Du, Y., Xie, M., and Jia, J. (2020). Stepped settlement: A possible mechanism for translational landslides. *Catena* 187, 104365. doi:10.1016/j.catena.2019.104365
- Du, Y., Xie, M. W., Jiang, Y. J., Liu, W. N., Liu, R. C., and Liu, Q. Q. (2019). Research progress on dynamic monitoring index for early warning of rock collapse [J]. *Chin. J. Eng.* 41 (04), 427–435. doi:10.13374/j.issn2095-9389.2019.04.002
- Duan, G. H., Niu, R. Q., Peng, L., and Fu, Jie. (2017). A landslide displacement prediction research based on optimizationparameter ARIMA model under the inducing factors[J]. *Geomatics Inf. Sci. Wuhan Univ.* 42 (04), 531–536. doi:10.13203/j.whugis.20140913
- Guo, Y. K., Zhang, S. A., Wang, J. J., Zhang, Q., and Xie, X. F. (2022). Feature variable selection combined with SVM for hyperspectral inversion of cultivated soil Hg content[J]. *Eng. Surv. Mapp.* 31 (01), 17–23. doi:10.19349/j.cnki.issn1006-7949.2022.01.003
- Jiang, S., Li, J. Y., Zhang, S., Gu, Q. H., Lu, C. W., and Liu, H. S. (2022). Landslide risk prediction by using GBRT algorithm: Application of artificial intelligence in disaster prevention of energy mining. *Process Saf. Environ. Prot.* 166, 386. doi:10.1016/j.psep.2022.08.043
- Jin, X. Z., Liu, Y., Yu, J., Wang, J. F., and Qie, Y. J. (2021). Prediction of outlet SO₂ concentration based on variable selection and EMD-LSTM network[J]. *Proc. CSEE* 41 (24), 8475–8484. doi:10.13334/j.0258-8013.pcsee.202589
- Li, B., Zhou, K., Ye, J., and Sha, P. (2019). Application of a probabilistic method based on neutrosophic number in rock slope stability assessment. *Appl. Sci. (Basel)*. 9, 2309. doi:10.3390/app9112309
- Li, H. W., Zhao, S. B., and Li, Z. (2021). Design and implementation of landslide early warning system based on multi-source monitoring data[J]. *Sci-Tech Dev. Enterp.* 2021 (12), 38–40. doi:10.3969/j.issn.1674-0688.2021.12.014

- Li, P. X. (2021). Application of mutual information in feature selection algorithm [J]. *Int. Core J. Eng.* 7 (12), 0082. doi:10.6919/ICJE.202112_7(12).0082
- Li, X. S., Li, Q. H., Hu, Y. J., Chen, Q. S., Peng, J., Xie, Y. L., et al. (2021). Study on three-dimensional dynamic stability of open-pit high slope under blasting vibration [J]. *Lithosphere* 2021, 6426550. doi:10.2113/2022/6426550
- Li, X. S., Peng, J., Xie, Y. L., Li, Q. H., Zhou, T., Wang, J. W., et al. (2022). Influence of high-temperature treatment on strength and failure behaviors of a quartz-rich sandstone under true triaxial condition [J]. *Lithosphere* 2022, 3086647. doi:10.2113/2022/3086647
- Lian, X. G., Li, Z. J., Yuan, H. Y., Hu, H. F., Cai, Y. H., and Liu, X. Y. (2020). Determination of the stability of high-steep slopes by global navigation satellite system (GNSS) real-time monitoring in long wall mining. *Appl. Sci.* 10 (6), 1952. doi:10.3390/app10061952
- Lin, X., Liu, Z. S., Gao, Y., and Wu, B. Y. (2019). Analysis of main controlling factors of oil production based on machine learning[J]. *China CIO News* 2019(12), 94–97+99. doi:10.3969/j.issn.1001-2362.2019.12.044
- Liu, G., Ye, L. X., Chen, Q. Y., Chen, G. S., and Fan, M. Y. (2022). Abnormal event detection of city slope monitoring data based on multi-sensor information fusion [J]. *Bull. Geol. Sci. Technol.* 41 (02), 13–25. doi:10.19509/j.cnki.dzdkq.2022.0060
- Liu, W. Y., Men, D. Y., Liang, J. F., and Wang, W. Z. (2012). Monthly load forecasting based on gray relational degree and least squares support vector machine[J]. *Power Syst. Technol.* 36 (08), 228–232. doi:10.13335/j.1000-3673.pst.2012.08.036
- Liu, Y., Xu, C., Huang, B., Ren, X. W., Liu, C. Q., Hu, B. D., et al. (2020). Landslide displacement prediction based on multi-source data fusion and sensitivity states. *Eng. Geol.* 271, 105608. doi:10.1016/j.enggeo.2020.105608
- Liu, Z. B., Shao, J. F., Xu, W. Y., Chen, H. J., and Zhang, Y. (2014). An extreme learning machine approach for slope stability evaluation and prediction. *Nat. Hazards (Dordr.)* 73 (2), 787–804. doi:10.1007/s11069-014-1106-7
- Liu, Z. X., Han, K. W., Yang, S., and Liu, Y. X. (2020). Fractal evolution mechanism of rock fracture in undersea metal mining. *J. Cent. South Univ.* 27, 1320–1333. doi:10.1007/s11771-020-4369-z
- Ma, K., Tang, C. A., Liang, Z. Z., Zhuang, D. Y., and Zhang, Q. B. (2017). Stability analysis and reinforcement evaluation of high-steep rock slope by microseismic monitoring. *Eng. Geol.* 218, 22–38. doi:10.1016/j.enggeo.2016.12.020
- Meng, Q. X., Wang, J., Tao, Z. G., Ren, D. Z., Zhang, G. C., Li, X. S., et al. (2021) 3D nonlinear analysis of stilling basin in complex fractured dam foundation, *Lithosphere* 2021, 2738130. doi:10.2113/2022/2738130
- Pang, J. (2019). Application of automatic monitoring system in high-risk slope monitoring project[J]. *Surv. World* 2019, 70–73. doi:10.3969/j.issn.1673-7563.2019.02.019
- Peng, M., Li, X. Y., Li, D. Q., Jiang, S. H., and Zhang, L. M. (2014). Slope safety evaluation by integrating multi-source monitoring information. *Struct. Saf.* 49, 65–74. doi:10.1016/j.strusafe.2013.08.007
- Pieraccini, M., Luzi, G., Mecatti, D., Noferini, L., and Atzeni, C. (2006). Ground-based SAR for short and long term monitoring of unstable slopes. *IEEE* 2006, 92–95. doi:10.1109/EURAD.2006.280281
- Qin, H. N., Ma, H., N., and Yu, Z. X. (2020). Analysis method of landslide early warning and prediction supported by ground-based SAR technology[J]. *Geomatics Inf. Sci. Wuhan Univer-sity* 45 (11), 1697–1706. doi:10.13203/j.whugis20200268
- Sakellariou, M. G., and Ferentinou, M. D. (2005). A study of slope stability prediction using neural networks. *Geotech. Geol. Eng. (Dordr.)* 23, 419–445. doi:10.1007/s10706-004-8680-5
- Salvoni, M., and Dight, P. M. (2016). Rock damage assessment in a large unstable slope from microseismic monitoring - MMG Century mine (Queensland, Australia) case study. *Eng. Geol.* 210, 45–56. doi:10.1016/j.enggeo.2016.06.002
- Šegina, E., Peterne, I. T., Urbančič, T., Realini, E., Zupan, M., Jez, J., et al. (2020). Monitoring surface displacement of a deep-seated landslide by a low-cost and near real-time GNSS system. *Remote Sens.* 12 (20), 3375. doi:10.3390/rs12203375
- Sulandri, S., Basuki, A., and Bachtiar, F. A. (2021). Metode deteksi intrusi menggunakan algoritme extreme learning machine dengan correlation-based feature selection. *J. Teknol. Inf. Dan. Ilmu Kompute* 8 (1), 103–110. doi:10.25126/jtiik.0813358
- Tuerxun, M., Zhao, M. J., Ning, C. B., and Kong, Q. H. (2021). Prediction of diesel engine exhaust emissions based on deep extreme learning machine[J]. *Sci. Technol. Eng.* 21 (36), 15646–15654. doi:10.3969/j.issn.1671-1815.2021.36.046
- Wang, L., Xu, H., Shu, B., and Tian, Y. Q. (2021). A multi-source heterogeneous data fusion method for landslide monitoring with mutual information and IPSO-lstm neural network[J]. *Geomatics Inf. Sci. Wuhan Univ.* 46 (10), 1478–1488. doi:10.13203/j.whugis20210131
- Wang, R. B., Zhang, K., Qi, J., Xu, W. Y., Long, Y., and Huang, H. F. (2022). A prediction model of hydrodynamic landslide evolution process based on deep learning supported by monitoring big data. *Front. Earth Sci. (Lausanne)* 10, 15. doi:10.3389/feart.2022.829221
- Wang, Z. W., Wang, L., Huang, G. W., Han, Q. Q., Xu, F., and Yue, C. (2020). Research on multi-source heterogeneous data fusion algorithm of landslide monitoring based on BP neural network [J]. *J. Geomechanics* 26, 575–582. doi:10.12090/j.issn.1006-6616.2020.26.04.050
- Xu, B., Huang, Q. S., and Qian, Y. D. (2022). Stability trends of Jinpingzi landslide: Numerical study. *Front. Earth Sci.* 1465, 940438. doi:10.3389/feart.2022.940438
- Xu, N. W., Li, B., Dai, F., Fang, Y. L., and Xu, J. (2016). Stability analysis of bedding rock slopes during excavation based on microseismic monitoring[J]. *Chin. J. Rock Mech. Eng.* 35 (10), 2089–2097. doi:10.13722/j.cnki.jrme.2015.0747
- Xue, J., and Shen, B. (2020). A novel swarm intelligence optimization approach: Sparrow search algorithm. *Syst. Sci. Control Eng.* 8 (1), 22–34. doi:10.1080/21642583.2019.1708830
- Yan, Y., Xiong, G. L., Zhou, J. J., Wang, R. H., Huang, R. H., Yang, M. W., et al. (2022). A whole process risk management system for the monitoring and early warning of slope hazards affecting gas and oil pipelines. *Front. Earth Sci. (Lausanne)* 9, 1336. doi:10.3389/feart.2021.812527
- Yi, T., Han, X., Weitao, Y., Wenbing, G., Erhu, B., Tingye, Q., et al. (2022). Study on the overburden failure law of high-intensity mining in gully areas with exposed bedrock. *Front. Earth Sci.* 10, 833384. doi:10.3389/feart.2022.833384
- Zeng, L., Lei, S. M., Wang, S. S., and Chang, Y. F. (2021). Ultra-short-term wind power prediction based on OVMD-SSA-DELM-GM model[J]. *Power Syst. Technol.* 45 (12), 4701–4712. doi:10.13335/j.1000-3673.pst.2021.0552
- Zhang, L. F., Chen, Z. H., Zhou, T. B., Nian, G. Q., Wang, J. M., and Zhou, Z., H. (2020). Multi-source information fusion and stability prediction of slope based on gradient boosting decision tree[J]. *J. China Coal Soc.* 45 (S1), 173–180. doi:10.13225/j.cnki.jccs.2020.0137
- Zhang, Y. G., Tang, J., Cheng, Y. M., Huang, L., Guo, F., Yin, X. J., et al. (2022). Prediction of landslide displacement with dynamic features using intelligent approaches. *Int. J. Min. Sci. Technol.* 32, 539–549. doi:10.1016/j.ijmst.2022.02.004
- Zhang, Y. H., Wang, Li, Shu, B., Haibo, H., and Long, L. (2020). “Application of an adaptive weighted estimation fusion algorithm in landslide deformation monitoring data processing,” in IOP Conference Series:Earth and Environmental Science, Changchun, China, 21–23 August 2020.
- Zhao, M. H., Liu, J. Y., Zhao, H., and Hou, J. C. (2022). Stability analysis of rock slopes based on MSDP criterion[J]. *Chin. J. Rock Mech. Eng.* 41 (01), 10–18. doi:10.13722/j.cnki.jrme.2021.0362